Synthesis and Physical Properties of Co-intercalated Layered Lanthanide Oxychlorides Li_xTHF_yLnOCl (Ln = Y, Lu)

Laurent Cario,* Sophie Delagrange, Florent Boucher, Eric Faulques, and Pierre Palvadeau

Institut des Matériaux Jean Rouxel, Laboratoire de Chimie des Solides, Laboratoire de Physique Cristalline, 2, rue de la Houssinière, BP 32229, 44322 Nantes Cedex 3, France

Received June 16, 2003. Revised Manuscript Received August 20, 2003

The LnOCl (Ln = Y, Lu) compounds have been successfully co-intercalated by Li and THF molecules. Infrared spectroscopy and atomic absorption spectroscopy agree with the formulation $Li_x(THF)_yLnOCl$ (Ln = Y, Lu; x ranging from 0.07 to 0.37). Characterizations by means of X-ray powder diffraction shows that these products are isotypic with the superconducting $Li_x(THF)_yMNCl$ (M = Zr, Hf) compounds (T_c up to 25.5 K). Band structure calculations performed for YOCl and ZrNCl indicate that the bottom of the conduction band is similar for both compounds. However, from magnetic susceptibility measurements none of the $Li_x(THF)_yLnOCl$ (Ln = Y, Lu) compounds were found to be superconducting down to 2 K.

Introduction

Except the well-known case of cuprates, very few superconductors exhibit a critical temperature (T_c) higher than 15 K. Among them, Chevrel phases, NbSn or NbGe alloys, niobium nitrides, or oxides ($Ba_{1-x}K_xBiO_3$) are the most typical (ref 1 and references therein). Recently, a new family of superconductor compounds has been identified. The layered chloronitrides of formula β-ZrNX (X = Cl, Br) were first reported by Juza and Friedrichsen[2] and further investigated by Yamanaka et al.[3] In 1996 superconductivity was reported in $Li_{0.16}ZrNCl$[3,4] and in 1998 superconductivity was observed in the homologous compound Li_xTHF_yHfNCl (THF for tetrahydrofuran) with a critical temperature of 25.5 K that represents one of the highest T_c for non-oxide materials.[5]

The layered materials β-MNX (M = Hf, Zr; X = Cl, Br) present trigonal lamellar structures of the rhombohedral SmSI structural type.[6] This structure is constituted by a stacking along the c axis of double layers [−X(MN−NM)X−] separated by a van der Waals gap in which various intercalations are possible (Figure 1). The isoelectronic compounds YOCl and LuOCl[7−9] crystallize in the rhombohedral SmSI or YOF structural types,[9,10] which means that they are isostructural (or present a very close structure) to β-ZrNCl (Figure 1). Moreover, the surrounding environment of the rare earths (three chlorine and four oxygen) in LnOCl and of Zr (or Hf) atoms in MNCl show very close bond distances (Figure 2). All these similarities made the intercalated species of YOCl and LuOCl very attractive as candidates for superconductivity. However, to our knowledge the low-temperature physical properties of LnOCl compounds that were successfully intercalated by alkaline metals or by molecules[11] were not reported. This prompted us to investigate the physical properties

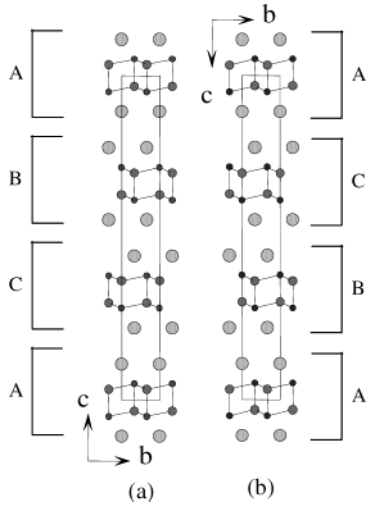

Figure 1. Comparison of the structural type of YOF (a) and SmSI (b).

* To whom correspondence should be addressed. E-mail: laurent.cario@cnrs-imn.fr.

(1) Ramakrishnan, T. V.; Rao CN. R. In *Superconductivity today*; Wiley Eastern Limited: New Dehli, 1992.
(2) Juza, R.; Friedrichsen, H. *Z. Anorg. Allg. Chem*. **1964**, *332*, 173−178.
(3) Yamanaka, S.; Kawaji, H.; Hohetama, K.; Ohashi, M. *Adv. Mater*. **1996**, *8*, 771−774.
(4) Kawaji, H.; Hohetama, K.; Yamanaka, S. *Chem. Mater*. **1997**, *9*, 2127−2130.
(5) Yamanaka, S.; Hohetama, K.; Kawaji, H. *Nature* **1998**, *392*, 580−582.
(6) Istomin, S. Ya.; Köhler, J.; Simon, A. *Physica C* **1999**, *319*, 219−228.
(7) Garcia, E.; Corbett, J. D.; Ford, J. E.; Vary, W. J. *Inorg. Chem*. **1985**, *24*, 494−498.
(8) Brixner L.; Ackerman, J. F.; Foris, C. M. *J. Lumin*. **1981**, *26*, 1−19.
(9) Meyer, G.; Staffel, T. *Z. Anorg. Allg. Chem*. **1986**, *532*, 31−36.
(10) Mann, A. W.; Bevan, D. J. M. *Acta Crystallogr. B* **1970**, *26*, 2129−2131.

10.1021/cm034494l CCC: $25.00
Published on Web 10/09/2003

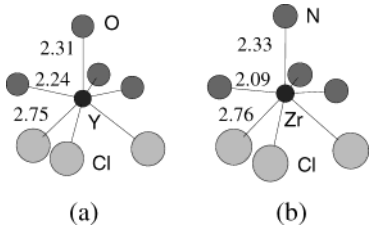

(a) (b)

Figure 2. Comparison view of the coordination polyhedra around Y^{3+} in YOCl (a) and Zr^{4+} in ZrNCl (b).

Table 1. Best Experimental Conditions To Prepare LnOCl

	LuOCl	YOCl
first step	30 h 270 °C	48 h 270 °C
second step	120 h 290 °C	240 h 330 °C

of Li_xTHF_yLnOCl (Ln = Y, Lu) species. The purpose of this paper is to report on the synthesis and co-intercalation by Li and THF of LnOCl (Ln = Y, Lu) compounds. The characterization of these compounds by means of X-ray powder diffraction, infrared spectroscopy, and temperature-dependent magnetic susceptibility will be detailed. Finally, an attempt to understand the physical properties on the basis of band structure calculations will be presented.

Experimental Section

Starting Materials. Ln_2O_3 and $LnCl_3{\cdot}6H_2O$ (Ln = Y, Lu) were purchased from Sigma, butyl-lithium and NH_4Cl from Aldrich. All solvents were dried and stored over molecular sieves prior to use. Solutions of butyl-lithium were diluted to 0.1 M concentration in hexane. Solutions of naphthalene lithium and sodium were prepared by dissolution of freshly distilled naphthalene and lithium or sodium in dried THF (tetrahydrofuran). After 20 h, the resulting dispersion was filtered to remove all impurities.

Synthesis. We have prepared the LnOCl (Ln = Y, Lu) compounds using the method reported by Corbett et al.[7] to synthesize YOCl. This method consists of reacting Ln_2O_3 with an excess of NH_4Cl in a two-step process.

First step:

$$12NH_4Cl + Ln_2O_3 \rightarrow 2(NH_4)_3LnCl_6 + 3H_2O + 6NH_3$$

Second step:

$$(NH_4)_3LnCl_6 + H_2O \rightarrow LnOCl + 3NH_4Cl + 2HCl$$

To prepare a pure powder of LuOCl and YOCl, we have performed the first step under a nitrogen stream and the second step under a nitrogen stream saturated by H_2O. To optimize the reaction time, the production of NH_3 (first step) and HCl (second step) was controlled by pH measurements of the water crossed by the gaseous flow. From our attempts the best experimental conditions are gathered in Table 1. LuOCl and YOCl were also successfully synthesized trough the second step only by heating directly $LnCl_3{\cdot}6H_2O$ instead of the reaction product of the first step. The resulting products LnOCl were dried under vacuum at 270 °C for 1 day and subsequently stored and used under a controlled atmosphere.

Alkali and THF co-intercalated compounds were obtained by immersing weighted quantities of LnOCl with different Me/LnOCl ratios (from 0.2 to 1.5) in 0.1 M solutions of naphthalene alkali metal (Me = Li, Na) in THF. After 72 h, the reacting products were filtered, rinsed with hexane, dried under vacuum at room temperature, and finally transferred into a drybox.

Chemical and X-ray Powder Diffraction Analyses. Chemical analyses of the host materials LnOCl were performed using a scanning electron microscope JEOL 5800SV. An INEL X-ray powder diffractometer equipped with a curved detector in Debye−Scherrer geometry (Cu Kα radiation) was used to measure the powder patterns. Prior to the measurement, the air-sensitive samples were loaded in Lindemann capillaries sealed under a nitrogen atmosphere. The percentage of intercalated lithium was obtained by atomic absorption spectroscopy, after dissolution in distilled water.

Infrared Spectroscopy. Infrared spectroscopy was performed at room temperature in the range 500−4000 cm^{-1} on a Nicolet 20 SXC FTIR spectrometer with a liquid nitrogen-cooled mercury−cadmium−tellurium detector. The spectral resolution was 4 cm^{-1}. Spectra were recorded using a diamond attenuated total reflectance apparatus (ATR). Samples in powder form were pressed at equivalent pressure on the diamond crystal. Tetrahydrofuran (THF) spectra were recorded from a single drop on the diamond surface. For each experiment, 500 spectra were collected and co-added. Reference spectra were obtained with the ATR apparatus open in air. The infrared beam was unpolarized.

Magnetic Susceptibility. Temperature-dependent magnetic susceptibilities were measured on a Quantum Design SQUID magnetometer on about 100 mg of each powders under magnetic fields of 10 and 100 Oe and are hereafter reported for the higher magnetic field only. Measurements were performed with the zero-field-cooled mode. The contribution of the gel caps containing the powders and the diamagnetic contribution of the core electrons were systematically subtracted from the measured signal.

Theoretical Calculations

The self-consistent band structure calculations were carried out using a scalar relativistic version of the full-potential linearized augmented plane waves (FLAPW) method as embodied in the WIEN2K code.[12] The exchange and correlation effect were treated within the density functional theory (DFT) using the generalized gradient approximation (GGA) suggested by Perdew et al.[13] For the calculation, the unit cell is divided into two parts: nonoverlapping atomic spheres and interstitial region. Inside the atomic spheres, the basis set is a linear combination of atomic-like wave functions and the l expansion was taken up to $l = 10$. In the interstitial part, plane waves (PW) are used with a cutoff parameter $R_{min} \times K_{max} = 7.0$, where R_{min} is the smallest sphere radius and K_{max} is the maximum wave vector value for the PW. A mixed LAPW and APW+lo (APW + local orbital) basis set has been used to expand the wave function.[12] The Brillouin-zone integration was performed with a modified tetrahedron method using 110 regular spaced irreducible k points.

Results

The host materials YOCl and LuOCl obtained using the reaction scheme proposed in ref 7 have been checked for purity and homogeneity. Analyses of both fine white powders, by means of X-ray energy-dispersive spectroscopy, revealed a rare earth-to-chlorine ratio close to 1 and confirmed the presence of oxygen. The X-ray powder diffraction diagrams, shown in Figures 3 and 4 for both

(11) Ford, J.; Corbett, J. *Inorg. Chem.* **1985**, *24*, 4120−4128.

(12) Blaha, P.; Schwarz, K.; Madsen, G. K. H.; Kvasnicka, D.; Luitz, J. *WIEN2K, An Augmented Plane Wave + Local Orbitals Program for Calculating Crystal Properties*; Karlheinz Schwarz, Techn. Universität Wien: Austria, 2001; ISBN 3-9501031-1-2.

(13) Perdew, J. P.; Burke, S.; Ernzerhof, M. *Phys. Rev. Lett.* **1996**, *77*, 3865−3868.

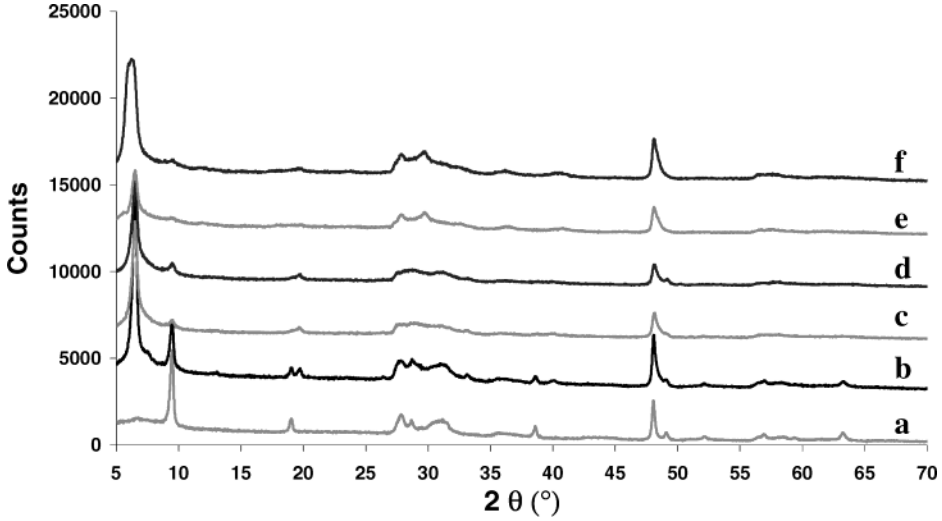

Figure 3. Experimental X-ray diffraction powder patterns of YOCl (a) and $Li_x(THF)_yYOCl$ (with (b) $x = 0.07$, (c) $x = 0.128$, (d) $x = 0.15$, (e) $x = 0.37$, and (f) $x = 0.23$), showing the increase of the *c* parameter after co-intercalation of Li and THF.

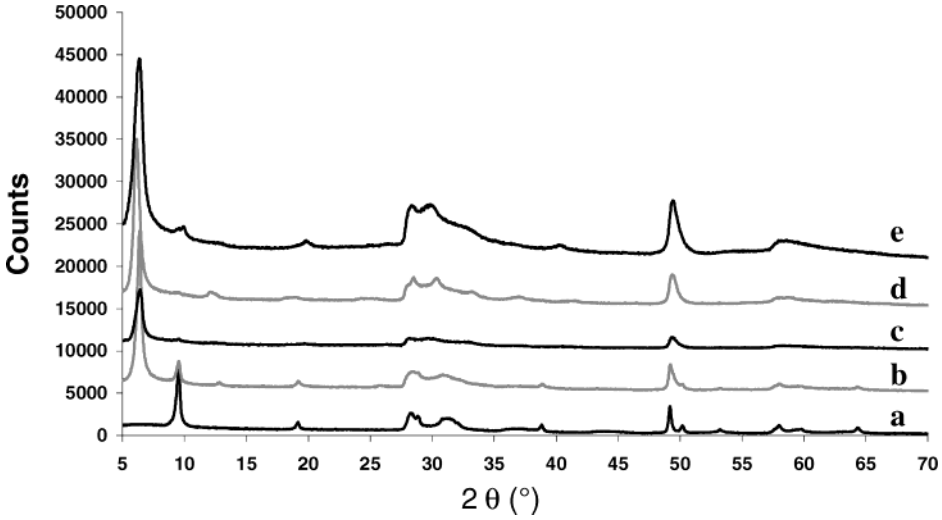

Figure 4. Experimental X-ray diffraction powder patterns of LuOCl (a) and $Li_x(THF)_yLuOCl$ (with (b) $x = 0.066$, (c) $x = 0.18$, (d) $x = 0.25$, and (e) $x = 0.26$), showing the increase of the *c* parameter after co-intercalation of Li and THF.

products, ascertain that the reactions yielded YOCl and LuOCl with a very good purity (>98%). A preferential orientation is clearly visible on the diagrams and the diffraction lines show an important width, which indicates that both compounds are poorly crystallized. Despite this poor quality of the diagrams, we could index the diffraction lines using the $R\bar{3}m$ space group, and we could refine the cell parameter values for LuOCl ($a = 3.704(1)$ Å, $c = 27.823(3)$ Å) and YOCl ($a = 3.788(1)$ Å, $c = 27.976(7)$ Å) that are in good agreement with those reported in the literature.[7,8] SmSI and YOF crystallize in the rhombohedral $R\bar{3}m$ space group and for the same compound both crystalline forms can only be distinguished by their diffracted intensity. The comparison of the diffracted intensities recorded for LnOCl (Ln = Y, Lu) with the simulated intensities obtained for the SmSI and YOF structure types revealed that the reactions yielded a mixture of both SmSI and YOF crystalline forms. Several authors had already reported this observation.[7,14]

In Figures 3 and 4 the X-ray diffraction powder diagrams of Li_xTHF_yLnOCl are compared to those of the host materials. For low initial naphthalene lithium/LnOCl ratios we observe that part of the host materials remain unintercalated after reaction. We could roughly estimate the fraction of remaining LnOCl from the X-ray diffraction data and we have indicated this ratio in Table 2. As expected upon intercalation, all diffraction patterns show a variation in position of the 00*l* diffraction lines, which attests to an increase of the interlayer parameter. On the other hand, the diffraction line (110) stays close to $2\theta = 48°$, which indicates that the in-plane parameter does not change. Table 2 gathers the refined in-plane parameters and interlayer spacing of the Li_xTHF_yLnOCl compounds. Comparing to the host materials, we note an increase of the interlayer spacing close to 4.30 Å, while the intercalation of lithium only would give an increase of 1 Å.[7] The large value of the interlayer distance obtained after intercalation indicates the co-intercalation of lithium and molecules of solvent (THF). The reaction is topotactic as the in-plane parameter remains unchanged. Using atomic absorption spectroscopy, we could measure the lithium intercalation ratios x = Li/LnOCl. As shown in Table 2, the reaction of LnOCl with naphthalene lithium yielded a series of co-intercalated compounds with x ranging from 0.07 to

(14) Song, K.; Kauzlarich, S. M. *Chem. Mater.* **1994**, *6*, 386−394.

Table 2. Lithium and THF Co-intercalation in YOCl and LuOCl: Chemical Analyses and Crystallographic Results[a]

initial ratio Li/LnOCl	Li_xTHF_yYOCl				Li_xTHF_yLuOCl			
	x	%	*a* (Å)	*d* (Å)	*x*	%	*a* (Å)	*d* (Å)
0	0		3.788(1)	9.323(2)	0		3.704(1)	9.274(1)
0.2	0.070(3)	20	3.777(3)	13.50(1)	0.066(1)	10.7	3.698(4)	13.88(1)
0.5	0.128(3)	4.8	3.780(5)	13.52(2)	0.180(4)	2	3.690(2)	13.78(1)
1.0	0.15(1)	8.2	3.780(5)	13.51(2)	0.250(3)	0	3.690(3)	14.41(4)
1.2	0.37(1)	0	3.780(4)	13.55(3)	0.260(3)	0	3.684(4)	13.91(7)
1.5	0.23(1)	0	3.779(2)	14.15(1)				

[a] This table gathers the number of lithium intercalated per LnOCl (*x*), the percentage of unintercalated host material (%), the in-plane parameter (*a*), and the interlayer spacing (*d*).

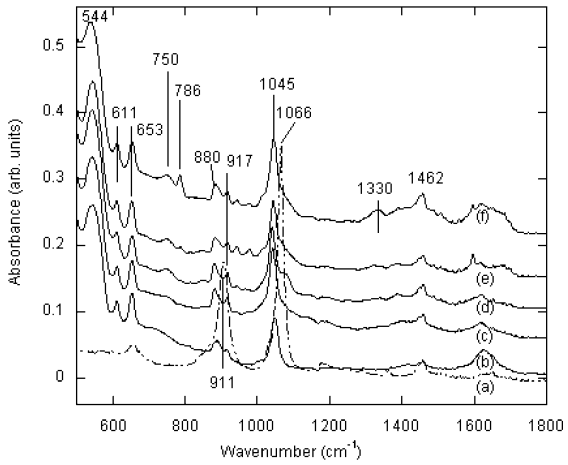

Figure 5. Infrared spectra of liquid THF and Li_xTHF_yYOCl between 500 and 4000 cm^{-1}, certifying the co-intercalation of THF in YOCl. (a) THF, (b) $x = 0.07$, (c) $x = 0.128$, (d) $x = 0.15$, (e) $x = 0.37$, and (f) $x = 0.23$.

0.37. The interlayer spacing seems independent of *x* apart from the cases of $Li_{0.23}(THF)_yYOCl$ and $Li_{0.25}(THF)_y$-LuOCl. For these latter compounds, the difference observed for the *c* parameter is likely related to a different orientation of the THF molecules in the host material, as already reported for $Li_x(THF)_yZrNCl$.[15] It is worth noting that there was no significant change in the color after intercalation.

To ascertain the co-intercalation of THF molecule within the van der Waals gap, we performed infrared spectroscopy measurements. Figure 5 displays the infrared spectra of THF and intercalated $Li_x(THF)_yYOCl$ in units of absorbance between 600 and 1800 cm^{-1}. Liquid THF shows intense bands at 653, 911, 1066, 1447, and 1459 cm^{-1} and at 2858, 2937, and 2972 cm^{-1} in the high-frequency range. In the free state, the THF molecule $(C_4H_8)O$ belongs to the C_{2v} point group. The representation of the vibrations is $\Gamma = 12A_1 + 5A_2 + 11B_1 + 5B_2$. A_1, B_1, and B_2 modes are IR-active. The IR-active ring vibrations themselves are represented by $\Gamma_{IR} = 4A_1 + 3B_1 + B_2$, so most of the observed bands stem from CH_2 groups. We notice that ring breathing, C−C and CH_2 in phase stretching should yield strong absorbance since A_1 species are totally symmetric. Experimentally, it is clear that most of the molecular THF lines appear in the intercalated compounds. This indicates that THF moieties are co-intercalated with Li in YOCl. Further, we notice that these vibrational lines undergo drastic changes in frequencies in $Li_x(THF)_y$-YOCl. The 911-cm^{-1} ring-breathing line splits into two well-resolved components around 880 and 917 cm^{-1}. The 1066-cm^{-1} C−C stretch line strongly downshifts toward 1047, 1044, 1041 1043, and 1045 cm^{-1} from $x = 0.07$ to $x = 0.37$. The position of the lines at 1447 and 1459 (CH_2 deformations) and 2937 cm^{-1} (CH_2 antisymmetric stretching) remains unchanged. The line at 2972 cm^{-1} splits into two lines at 2961 and 2981 cm^{-1}, whereas that at 2858 cm^{-1} strongly upshifts toward 2887 cm^{-1}. Spectral changes of THF infrared bands in $Li_x(THF)_y$-YOCl derivatives confirm that THF moieties are not only intercalated between the layers but also that they are chemically bonded. The bonding nature is revealed by the degeneracy removal of the free molecular THF vibrations and indicates strong interactions with the lattice whose symmetry is reflected by the spectral THF changes. This is also apparent in the 2800−3100-cm^{-1} region, which is characteristic of CH_2 symmetric and antisymmetric stretching molecular modes that are vibrating at shifted frequencies in intercalates. The IR lines, which can be ascribed to the phonons of the Li_x-YOCl matrix, are located at 544, 611, 750, and 786 cm^{-1}. The latter one appears only for $x = 0.23$ and 0.37, while the strong one at 544 cm^{-1} is downshifted to 538 cm^{-1} for $x = 0.23$. These bands may be directly related to lithium insertion. The other lines do not vary in position and intensity and therefore should be identified as vibrations of the YOCl layers. The overall IR results indicate that electronic changes occur during lithium and THF insertion.

To gain some insight into the electronic structure of YOCl, we have carried out a FLAPW calculation for the trigonal structure reported by Meyer et al.[9] Figure 6 gives the total and partial density of states (DOS) obtained with this method. The low-lying energy band is coming mainly from the O 2p and Cl 3p states. We found bands, which were higher in energy, with mainly cationic character, namely, the yttrium d states. An energy gap of the order of 4 eV is opened between the anionic p-bands and the cationic d-bands. As expected, the calculation predicts an insulating behavior with the Fermi level lying within this energy gap.

Assuming a rigid band model, extra electrons added upon intercalation of alkali metals in the YOCl host structure would fill the lower part of the d bands. This makes these bands of special interest and we should go deeper into their analysis. As shown in Figure 2, yttrium atoms are sitting in a distorted octahedron (made of three oxygen atoms at 2.229 Å and three chlorine atoms at 2.762 Å), which is capped by extra oxygen at 2.348 Å. Consequently, the usual splitting of the d bands in t_{2g} and e_g encountered for transition metals in octahedral coordination is furthermore complicated in the present case. In fact, the band disper-

(15) Ohashi, M.; Uyeoka, K.; Yamanaka, S.; Hattori, M. *Chem. Lett.* **1990**, 93−96.

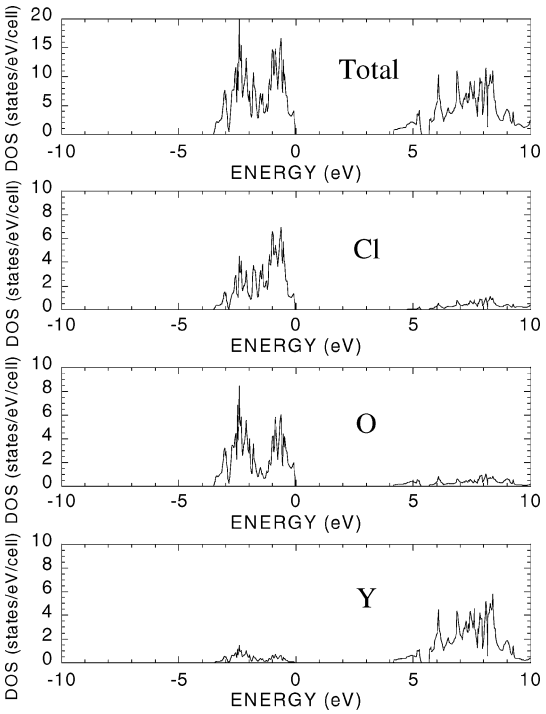

Figure 6. Drawing of the total and partial density of states (DOS) calculated for YOCl with the structure proposed in ref 9.

sions represented in Figure 7 indicate that the d block of Y can be decomposed into three parts. Considering first the $Z-\Gamma$ high-symmetry line, we find at high energy ranging from 9.1 to 9.3 eV four bands having mainly $d_{x^2-y2} + d_{xy}$ Y character ($Z = 2$ for the primitive cell). Those states are mixed by σ^* interaction with the $p_x + p_y$ O states. Ranging from 5.7 to 6.5 eV, we find four other bands with mainly Y $d_{xz} + d_{yz}$ character and hardly no O p character. At Γ, due to the $\bar{3}m$ point group symmetry (D_{3d}), theses 8 states can be decomposed into $2E_u$ and $2E_g$ irreducible representations. The two bands with mainly Y d_{z^2} character are found within the energy range 6.2−6.7 eV and can be decomposed at Γ in A_{1g} and A_{2u} irreducible representations. Within the Brillouin zone, the Y d_{z^2} block is slightly dispersed over 2 eV, the Y $d_{xz} + d_{yz}$ block is spread over 3.1 eV, and the largest dispersion is observed for the Y $d_{x^2-y^2} + d_{xy}$ block with 5.2 eV. The dispersion scheme of the d bands is well-explained by the lamellar character of the structure and the σ or π type bonding into the layer. However, at the bottom of the conduction band, we observe a band ranging from 4.1 to 5.3 eV that is separated from the others by an energy gap of about 0.3 eV and is spread over less than 1.2 eV. Surprisingly, at Γ, this state does not have a main Y d character. This situation is completely different than what is found by different band structure calculations for ZrNCl.[6,16] Therefore, a comparison between the band structures of YOCl and ZrNCl is useful for understanding this discrepancy.

Figure 7 presents in the lower part the dispersion of the bands calculated for ZrNCl using the same method. To ease the comparison, the bands of ZrNCl have been plotted with the same energy reference fixing the Cl 1s energy of ZrNCl at the value found for YOCl. Compared to YOCl, the energy gap found in ZrNCl between the conduction and the valence bands drop drastically. At first glance, the metal d bands are found at higher energy in YOCl, leading to a stronger ionic character in this compound. Consequently, the d bands of Y are spread over less than 5.2 eV while the d bands of Zr are spread over more than 7 eV. In both compounds the d-block shows the same features but the discrepancy between their band structures comes from the relative position of one anionic band relative to the d-block. As shown in Figure 8, at Γ in ZrNCl we find two anionic states lying within the d-block and located at 9.7 (A_{2u}) and 6.5 eV (A_{1g}). The highest of these states is mainly Cl 4s in character while the lowest is mainly N 3s in character. In YOCl, at Γ the Cl 4s states are still visible at 9 eV and can be decomposed in A_{2u} irreducible representation (see Figure 8). However, the second anionic state, mainly O 3s at Γ (A_{1g}), is no longer found within the d-block and lies below this block at 5.2 eV. This differs from ZrNCl in which the lowest A_{1g} state (at Γ) is mainly Zr d_{z^2} in character. Therefore, at Γ, we can easily interpret the character inversion of the A_{1g} states by the relative position of the 3s anionic band with respect to the metal d_{z^2} band.

In YOCl, the character of the lowest band (A_{1g} in Γ) evolves throughout the Brillouin zone due to a large number of avoided crossings. The main character is anionic at Γ but cationic at Q. As shown in Figure 7, for both compounds YOCl and ZrNCl the bottom of the conduction band (Q) is made of similar metal $d_{x^2-y^2} + d_{xy}$ states mixed with anion (N or O) $p_x + p_y$ states. Upon intercalation the states at the bottom of the d-band block would play a major role in the electronic properties.

The structural and electronic similarities between YOCl and β-ZrNCl urged us to investigate the magnetic properties of the co-intercalated species Li_xTHF_yLnOCl, hoping to find superconducting behavior. Figures 9 and 10 give the thermal dependence of the molar susceptibility obtained for the co-intercalated compounds Li_xTHF_yYOCl ($x = 0$, 0.128, 0.15, 0.23, and 0.37) and Li_xTHF_yLuOCl ($x = 0$, 0.066, 0.18, 0.25, and 0.26). For both synthesized compounds YOCl and LuOCl, the molar susceptibility is temperature-independent between 2 and 300 K. No paramagnetic deviation is observed at low temperature, which attests to the high purity of both products. For $Ln^{+3}O^{-2}Cl^-$ we expect diamagnetic behavior due to the core electrons. For LuOCl, the molar susceptibility obtained after removing the calculated core electron diamagnetism (see Figure 10) is very close to zero, which shows that the product is really diamagnetic. In contrast, for YOCl the molar susceptibility is significantly above zero ($\chi = +2.6\ 10^{-4}$ emu/mol) and the product is not diamagnetic. A small oxygen deficiency, as evidenced in $YO_{1-x}Cl$ by Ford et al.,[7] could explain this discrepancy, as it would fill the conduction band and lead to Pauli-like behavior.

For the co-intercalated compounds $Li_x(THF)_yLnOCl$ (Ln = Y, Lu) we observe a positive molar susceptibility that is almost temperature-independent between 2 and 300 K (Figures 9 and 10). No transition from a paramagnetic state to a pure diamagnetic state is observed: the co-intercalated compounds $Li_x(THF)_yLnOCl$ (Ln = Y, Lu) are not superconducting.

(16) (a) Felser, C.; Seshadri, R. *J. Mater Chem.* **1999**, *9*, 459−464. (b) Fuertes, A.; Vlassov, M.; Beltran-Porter, D.; Alemany, P.; Canadell, E.; Casan-Pastor, N.; Palacin, R. *Chem. Mater.* **1999**, *11*, 203−206.

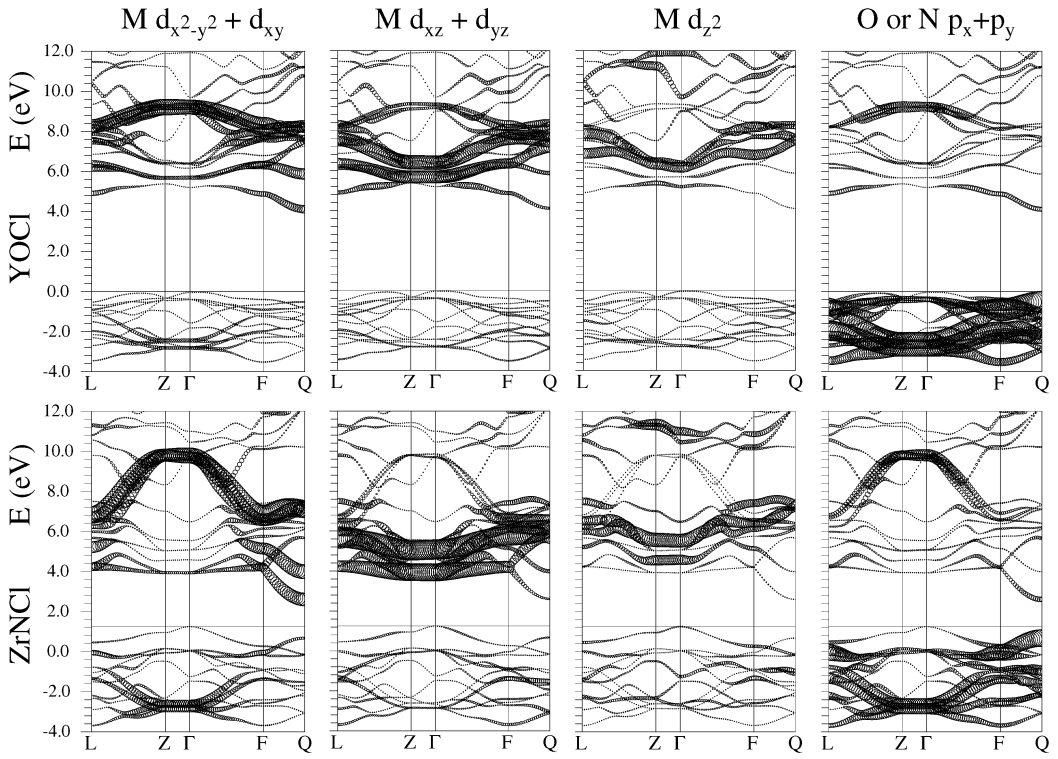

Figure 7. Comparison of the band structures of YOCl (upper part) and ZrNCl (lower part). The atomic characters are highlighted using the fat band representation. The high-symmetry points are L (0 $^1/_2$ 0), Z ($^1/_2$ $^1/_2$ $^1/_2$), Γ (0 0 0), F ($^1/_2$ $^1/_2$ 0), and Q ($^1/_3$ $^2/_3$ 0).

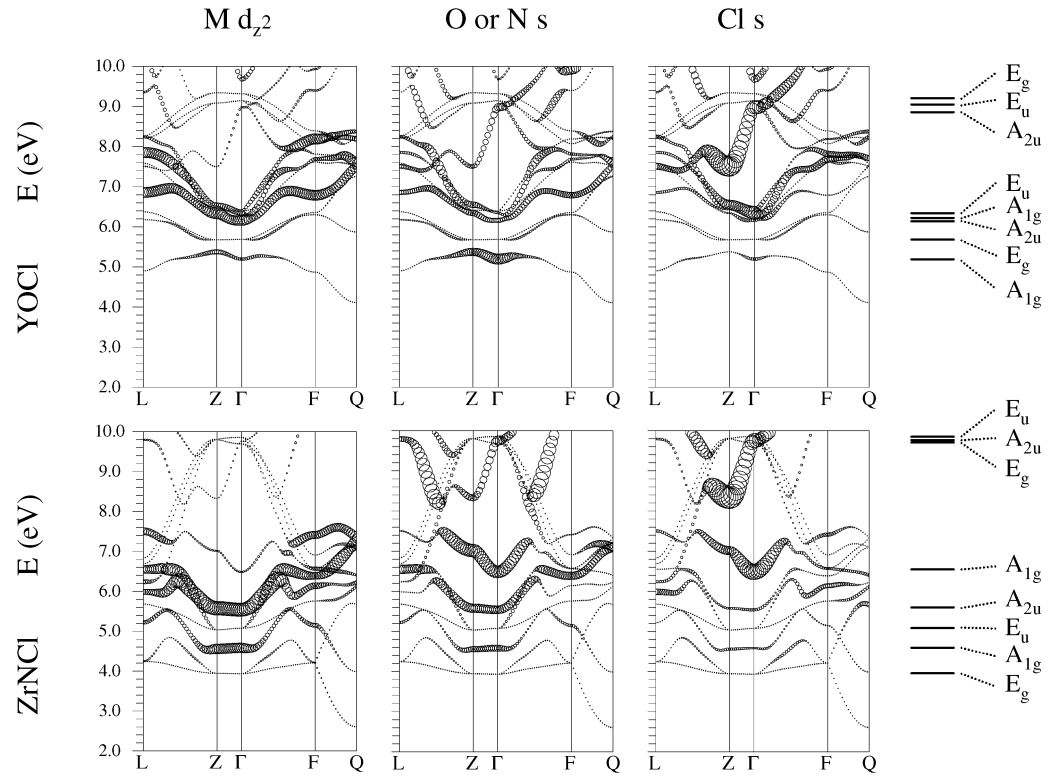

Figure 8. Comparison of the d-band blocks of YOCl (upper part) and ZrNCl (lower part). The fat band representation is used to highlight the M d_{z^2}, N (or O) 3s, and Cl 4s atomic characters. The high-symmetry points are L (0 $^1/_2$ 0), Z ($^1/_2$ $^1/_2$ $^1/_2$), Γ (0 0 0), F ($^1/_2$ $^1/_2$ 0), and Q ($^1/_3$ $^2/_3$ 0). On the right part, the irreducible representation is given for the states at Γ.

The positive temperature-independent molar susceptibility observed for the co-intercalated compounds recall the Pauli paramagnetism typical of metallic compounds. If so, the susceptibility χ_p measured for the $Li_x(THF)_y$-LnOCl (Ln = Y, Lu) derivatives suggest that the density of states at the Fermi level $n(E_f)$ is ranging from 58 to 300 states/eV/formula unit according to the relationship $\chi_p = \mu_B{}^2 n(E_f)$ obtained for the free electron gas. This is too high compared to what is calculated with the LAPW method for a d-band block of yttrium in YOCl, which is of the order of 2 states/eV/formula units. Such a discrepancy between the measured and the calculated

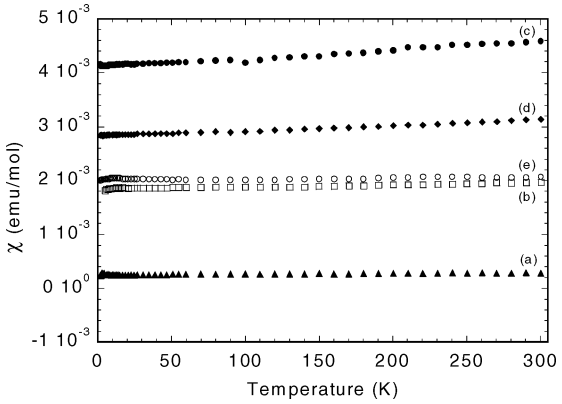

Figure 9. Thermal dependence of the molar magnetic susceptibly measured for nonintercalated compound YOCl (a) and for the co-intercalated compounds $Li_x(THF)_yYOCl$ with x = 0.128 (b), 0.15 (c), 0.23 (d), and 0.37 (e).

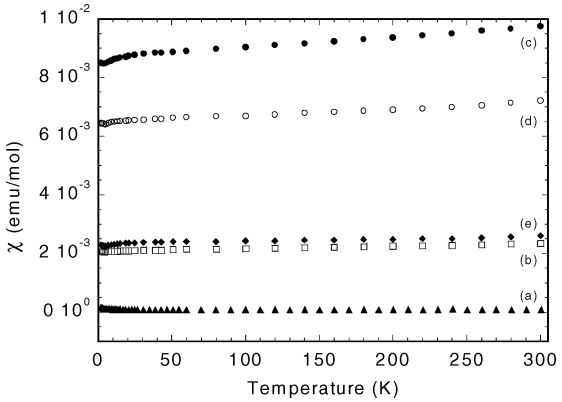

Figure 10. Thermal dependence of the molar magnetic susceptibly measured for the nonintercalated compound LuOCl (a) and for the co-intercalated compounds $Li_x(THF)_yLuOCl$ with x = 0.066 (b), 0.18 (c), 0.25 (d), and 0.26 (e).

values could be explained by the presence of strong Coulomb interactions between itinerant electrons (i.e., a Stoner instability).

Discussion

Both compounds LnOCl (Ln =Y, Lu) and MNCl (M = Zr, Hf) are isotypic and isoelectronic and display some similarities in their electronic band structures close to the Fermi level. One would expect similar physical properties. But none of the $Li_x(THF)_yLnOCl$ (Ln = Y, Lu) products are superconducting, while the $Li_x(THF)_yMNCl$ (M = Zr, Hf) compounds show a superconducting transition below 25 K.

Besides the mentioned similarities we should point out strong differences between both kinds of compounds that could play an important role in explaining their behavioral discrepancy. First, in ZrNCl and HfNCl there are van Hove singularities,[6,16] which are missing in YOCl. Second, the band gap size is quite different between these compounds, which will have a huge impact on most physical properties. Finally, above the superconducting transition Yamanaka et al. measured a susceptibility of the order of 10^{-6} emu/g for the chloronitrides $Li_{0.48}(THF)_yMNCl$ and $Li_{0.16}(PC)_yMNCl$ (M = Zr, Hf).[5] From this value we can roughly estimate the density of states at the Fermi level to be of the order of 7 states/eV/formula unit. This is in good agreement with the density of states of the order of 2 states/eV/formula unit calculated with the LMTO or EHTB techniques for the d-block bands of Zr or Hf in the chloronitrides.[6] Consequently, above the superconducting transition the $Li_x(THF)_yMNCl$ (M = Zr, Hf) compounds behave as normal metals and exhibit a temperature-independent susceptibility with hardly any sign of electronic correlations. In contrast, magnetic data gathered for the co-intercalated oxychlorides suggest that they behave as strongly correlated metals.

The strong increase of the Coulomb interactions between itinerant electrons observed on going from chloronitrides to oxychlorides is not so surprising. Oxides are known to be more ionic than nitrides and we may expect a narrowing of the d-block band for the oxychlorides compared to that of the chloronitrides. This is well-supported by band structure calculations that show that the lower d bands are spread over 3 eV in the chloronitrides while over less than 1.2 eV for the oxychlorides. Such a narrowing of the d band could favor the appearance of Coulomb interactions. We are not surprised to observe a Stoner type enhancement of the Pauli paramagnetism susecptibility in the oxychlorides. Moreover, we think that these strong Coulomb interactions could easily explain the lack of superconductivity for the oxychlorides $Li_x(THF)_yLnOCl$ (Ln = Y, Lu).

CM034494L